J Therm Spray Tech (2017) 26:1095–1103
DOI 10.1007/s11666-017-0526-9

PEER REVIEWED

The Influence of Composition and Microstructure on the Abradability of Aluminum-Based Abradable Coatings

Jianming Liu[1,2] · Yueguang Yu[1,2] · Tong Liu[2] · Xuying Cheng[1,2] · Jie Shen[2] · Changhai Li[2]

Submitted: 29 September 2016 / in revised form: 12 December 2016 / Published online: 27 January 2017

Abstract Five kinds of commercial aluminum-based abradable coatings including AlSi, Al-hBN, AlSi-polyester, AlSihBN and Al-AlSi-hBN were fabricated to perform parallel abradability tests rubbed against Ti6Al4V dummy blades at high temperature up to 450 °C and high velocity up to 300 m/s conditions. AlSi coating, which contains no additional secondary filler, only showed acceptable abradability at medium incursion rate under 450 °C, and severe blade wear or coating transfer to blade tip occurred at low and high incursion rates. Other four coatings which contain secondary fillers performed far beyond AlSi coating. It was found that not only the amount added but also the diameter of secondary fillers plays an important role in coating abradability. For the similar filler addition level, Al-hBN and Al-AlSi-hBN coatings which contain fine filler performed much better than AlSi-hBN coating with coarse filler. Shorter filler spacing in the fine filler samples is concluded to be the reason for better abradability.

Keywords abradable coating · aerospace · aluminum alloys · high temperature wear · microstructure · sliding wear testing

Introduction

Thermal spray abradable coatings have been widely applied in aero-engines for over 50 years (Ref 1). Abradable coatings can be easily rubbed in by rotating parts such as blades and mate labyrinth teeth to protect them from wearing and minimize the clearance between stationary and rotational parts like rotor and stator, hence maintaining engine efficiency. Abradable coatings can serve in extreme environments with a high velocity up to 650 m/s and a high temperature up to 1200 °C (Ref 2, 3). Due to the lack of coating design theory for the serious working environments, the development of abradable coatings was mainly based on experience, and even being considered as a 'black art' (Ref 4).

Various methods have been employed and studied to evaluate coating properties, such as scratching tests (Ref 5), mechanical property tests with freestanding coating samples (Ref 6), residual stress tests (Ref 7), numerical method (Ref 8) and high-temperature and high-speed rubbing tests. It is believed that high-temperature and high-speed rubbing test can mostly simulate the turbine working condition and estimate coating abradability being comparable to engine test. Therefore, a number of test rigs with a capability at high speed and/or high temperature have been developed by abradable material manufacturers, engine companies and research organizations. By the help of those test rigs, many experimental data of coating abradability were obtained, and the data promote further coating development and applications, as well as a better understanding on coating rubbing mechanisms (Ref 9-16).

To meet those of clearance control requirements in advanced turbines, over 50 different thermally sprayed abradable coatings have been used in service, and more innovative abradable coatings for high-temperature applications are still on developed (Ref 17, 18).

At the low- and medium-temperature sections of aero-engine compressor, the rotor parts are made of titanium alloys having poor wear properties; hence, a soft abradable coating should be selected (Ref 2, 19). Aluminum-based abradables, in which Al/Al-alloy matrix has lower elastic

✉ Jianming Liu
Liu1983.2.1@163.com

[1] Northeastern University, Shenyang 110819, China

[2] Beijing General Research Institute of Mining and Metallurgy, Beijing 100160, China

modulus and lower melting points, compared with the titanium alloys, were selected as the counterpart of titanium rotors (Ref 2, 10, 19). Pure aluminum was directly used as the abradable coating in the early stage, leading to a problem of serious aluminum transfer to the rotors. Then, an aluminum silicon (AlSi) alloy matrix was considered, and secondary fillers like polyester, graphite and hexagonal boron nitride (hBN) were also added to the matrix.

A few of studies on the abradability of aluminum-based abradables have been reported. Stringer and Fois (20) studied the transfer behavior of AlSi-hBN coating using a high-speed test rig at the room temperature. Xue (21) observed the transfer behavior between Ti6Al4V blade and an aluminum hexagonal boron nitride abradable coating during high-speed rubbing at the room temperature. Bounazef investigated the rubbing phenomena on AlSi-BN-bounding coating at high-speed and high-temperature conditions (Ref 22). Those studies mainly focused on a single coating and its general rubbing behaviors for understanding mechanisms of aluminum-based abradables. So far, the difference in coating abradability and rubbing mechanism of different aluminum-based abradable coatings has not been well studied yet, even several kinds of aluminum-based abradables are already on using in the compressor section of aero-engines, nowadays.

To help making better coating selection and developing aluminum-based abradable coatings, it is necessary to make comparative study of different abradable coatings tested in similar or identical conditions. In this study, five typical commercial aluminum-based abradable coatings were selected for abradability testing by a high-temperature and high-speed rig. The coating abradability related to their chemical compositions and microstructures were investigated.

Experiments

Materials and Samples

Five aluminum-based abradable coatings were selected in the present work. The coatings were all deposited by atmospheric plasma spray. The nominal composition and size distribution of feedstock powders of the abradable coatings are listed in Table 1. Al-12Si eutectic alloy feedstock powders were manufactured by gas atomizing. AlSi-polyester feedstock powders were fabricated by blending Al-12Si powders and polybenzoate powders. Mechanical cladding method was used to produce Al-hBN, AlSi-hBN and Al-AlSi-hBN feedstock powders. All feedstock powders are prepared by Beijing General Research Institute of Mining and Metallurgy (Beijing, China).

Coating samples for abradability test were sprayed onto 40 mm × 60 mm × 8 mm 316L stainless steel plates by a F6 plasma torch (GTV Verschleiss-schutz GmbH, Germany). All samples of each coating were deposited from

Table 1 Composition, size distribution of feedstock powders and coating hardness

Coating name	Nominal composition of feedstock powder, wt.%	Powder size distribution, μm	Coating hardness (R15Y)	
			Average value	SD
AlSi	Al-12Si	42-98	85	1.34
Al-hBN	Al + 20hBN + 6acrylate	25-105	32	2.65
AlSi-polyester	Al-12Si + 40 polybenzoate	10-124	68	1.48
AlSi-hBN	Al-12Si + 20hBN + 8acrylate	16-250	63	1.79
Al-AlSi-hBN	Al + 40Al-12Si + 20hBN + 6acrylate	23-105	73	1.86

Table 2 Key spray parameters for 5 abradable coatings

Coating name	Argon flow rate, slpm	Hydrogen flow rate, slpm	Powder feed rate, g/min	Current, A	Power, kw	Spray distance, mm
AlSi	47	7	70	600	36	125
Al-hBN	40	3.5	40	400	23	110
AlSi-polyester	70	8	25	420	30	90
AlSi-hBN	70	5	40	390	28	120
Al-AlSi-hBN	40	3.5	40	400	23	110

the same lot of powder and the same run. The key spray parameters for each kind of coating are listed in Table 2. The coating thickness was controlled in a range of 2.0-2.2 mm. Hardness of as-sprayed coatings was measured using Rockwell R15Y hardness scale (600 MRD-S, WOLPERT, China). Samples for hardness measurement were grounded by 120# sandpaper on a polishing/grind machine. The average values and the standard deviation of 5 indentation readings for each coating are given in Table 1. All abradability tests were accomplished on the as-sprayed coatings.

Fig. 1 Photograph of the dummy blades

Ti-6Al-4V titanium alloy was selected as the rotor material. The rotor test samples will rub into the aluminum-based abradables. The dummy blades with a tip dimension of 0.7 mm × 10 mm × 3 mm were fabricated from a rolled Ti-6Al-4V plate. An image of dummy blades is presented in Fig. 1.

Microstructure Characterization of Coating

The as-sprayed coating samples were sectioned by wire-electrode cutting machine and mounted using epoxy resin by a vacuum impregnation system (Cast N 'Vac 1000, BUEHLER, Illinois, USA). The specimens were grounded off more than 1.5 mm with 80#sandpaper to get rid of the cutting effected zones before further fine grounding and polishing. A FEI Quanta 200 model scanning electron microscope (SEM, FEI, Oregon, USA) was used to observe microstructure of coating. The average area fraction value of metallic phase on the coating section in SEM picture was calculated by using a software ImageJ (National Institutes of Health, USA), based on five fields of view chosen randomly at 100× magnification.

Abradability Test and Evaluation Method

The abradability tests were carried out on a high-temperature and high-speed abradability test rig (BKV-HVT 300/800 model, Beijing General Research Institute of Mining and Metallurgy, China). The sketch map and a photograph of the rig are shown in Fig. 2 and 3, respectively.

A high-speed spindle with a maximum speed of 15,000 rpm was used to drive a 475-mm-diameter disk. A dummy blade and a balancing blade were symmetrically mounted to the rim of the disk, and the dummy blade tip

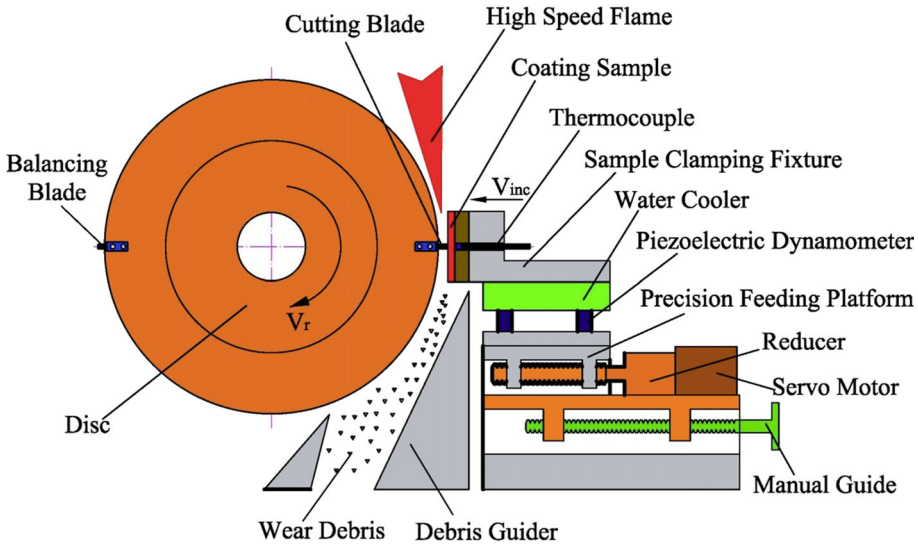

Fig. 2 Schematic of high-temperature and high-speed abradability test rig

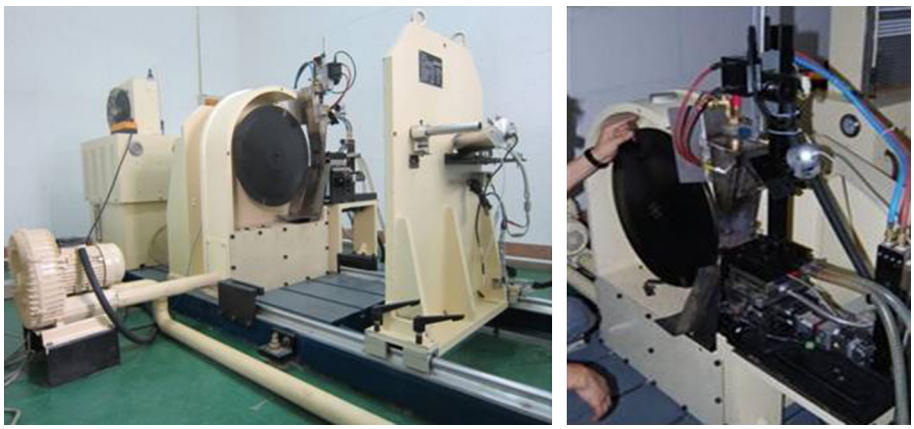

Fig. 3 Photograph of BGRIMM BKY-HVT300-800 abradablity test rig

Table 3 Abradability test parameters

Test number	Coating material	Blade tip velocity, m/s	Incursion rate, μm/s	Set incursion depth, μm	Temperature, °C
1	AlSi	300	5	1000	25
2			5		450
3			50		
4			480		
5	Al-hBN		5	1000	25
6			5		450
7			50		
8			480		
9	AlSi-polyester		5	1000	25
10			5		325
11			50		
12			480		
13	Al-AlSi-hBN		5	500	25
14			5		450
15			50		
16			480		
17	AlSi-hBN		5	500	25
18			5		450
19			50		
20			480		

protrudes 5 mm out of the disk. With this configuration, a maximum blade tip velocity of 350 m/s can be achieved. Abradable coating samples were fixed onto a stepper-motor-driven platform. The incursion rate of the coating sample to the rotor can be precisely controlled in a range of 5 to 1000 μm/s. A high-speed flame generated by an oxygen-acetylene burner was used to heat the coating from the rear of the substrate, and a pyrometer was held toward the center of coating surface to monitor and help adjusting the coating temperature. For the present rig setting, the coating can be heated up to 800 °C with corresponding blade tip velocity of 300 m/s. A 3-axis force sensor is mounted to the specimen stage to record the vertical and tangential cutting force on the coating. The sensor and the precision feeding platform are insulated from the hot section by a water-cooled plate.

Abradability of each coating was tested under both of the room and the maximum coating service temperatures. The blade tip velocity was set as 300 m/s for all tests. Three levels of incursion rates were used, and they are 5, 50 and 480 μm/s, respectively. Only the 5 μm/s tests were applied for both of the room- and high-temperature conditions. The selected abradability test parameters are given in Table 3.

In this study, coating abradability is quantitatively evaluated by a ratio of the blade wear to coating incursion depth (IDR) which was developed by Metco (Ref 10). IDR is calculated according to the percentage of blade height change to the precise incursion depth into the coating (wear depth). An IDR value close to zero means an improved abradability of the seal system. The ratio is positive when blade wear was predominant; otherwise, negative value means that adhesive transferred from the coating to the tip. The blade height change was measured using a caliper. The wear depth was not measured directly using a micrometer or profile meter because the reference surfaces were often distorted or damaged so that the precision was too low. Instead, the coating wear scar depth was determined by measuring the wear scar length and converting this to depth using geometry. The formula is given as follows:

$$I = R - \sqrt{R^2 - \left(\frac{L}{2}\right)^2}$$

where I is the coating wear scar depth, R rotor radius, L coating wear scar length.

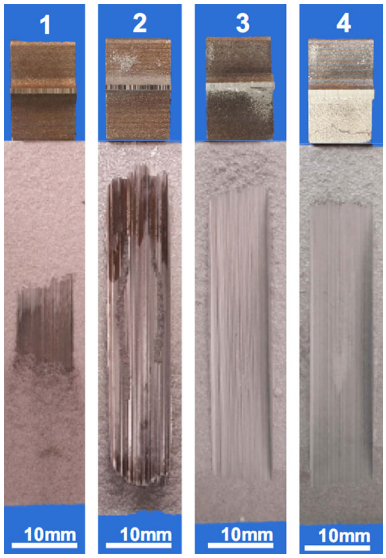

Fig. 4 Photographs of the blade tip and AlSi coating surface after abradability test, corresponding to the test conditions of number 1-4 as listed in Table 3

Results and Discussion

Abradability Test Results

Figure 4 presents the surface morphology of the dummy blade and AlSi coating after abradability tests, and the testing number is marked on the picture. The T6Al4V dummy blade can hardly cut into the AlSi coating at the room temperature, only short black wear tracks observed. The black color of wear track indicated severe blade material transfer to the coating. With the increase in temperature, the abradability of AlSi coating was improved obviously. The dummy blade can cut into AlSi coating at the same incursion rate and blade tip velocity as at the room temperature; but a longer wear track was made although blade material still transferred to coating. As the incursion rate was increased to 50 and 480 μm/s,no more obvious blade wear or blade material transfer to the coating

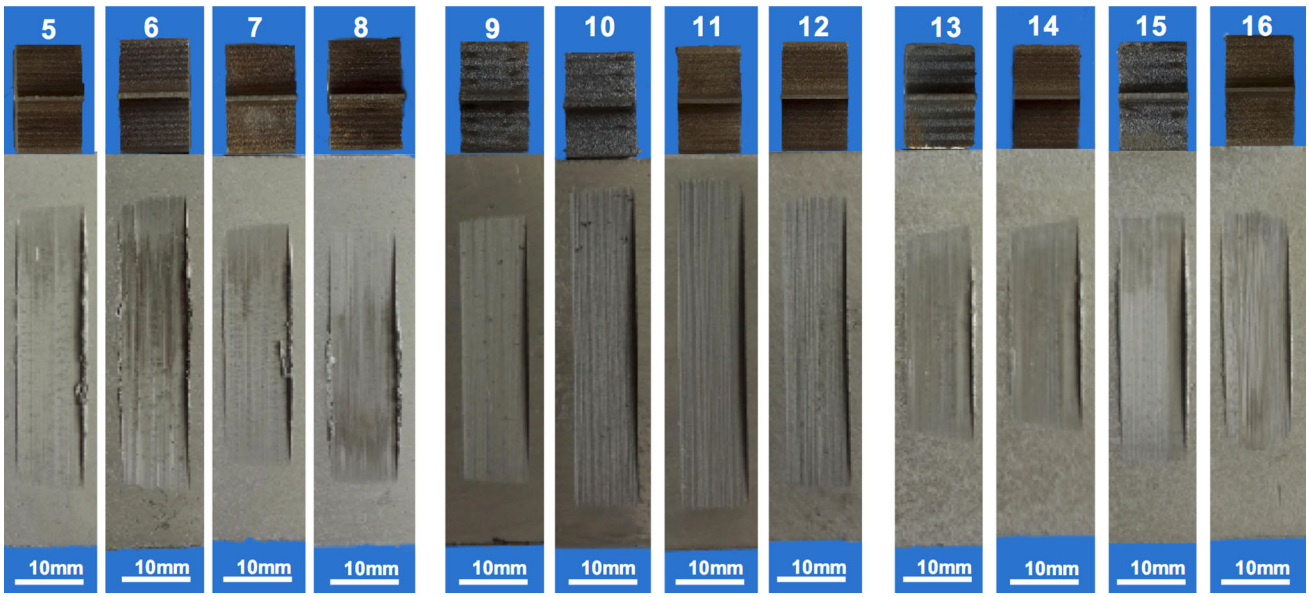

Fig. 5 Photographs of blade tip and coating surface of Al-hBN, AlSi-polyester and Al-AlSi-hBN coatings after abradability test, corresponding to the test conditions of number 5-16 as listed in Table 3

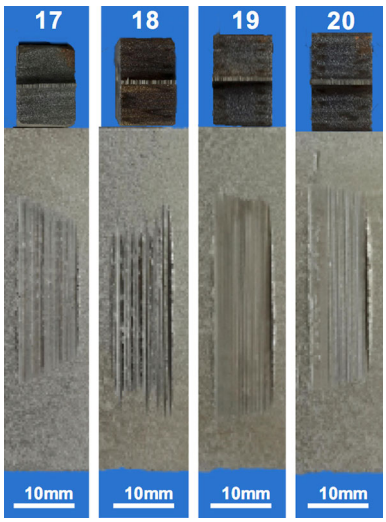

Fig. 6 Photographs of blade tip and coating surface of AlSi-hBN coating after test, corresponding to the test conditions of number 17-20 as listed in Table 3

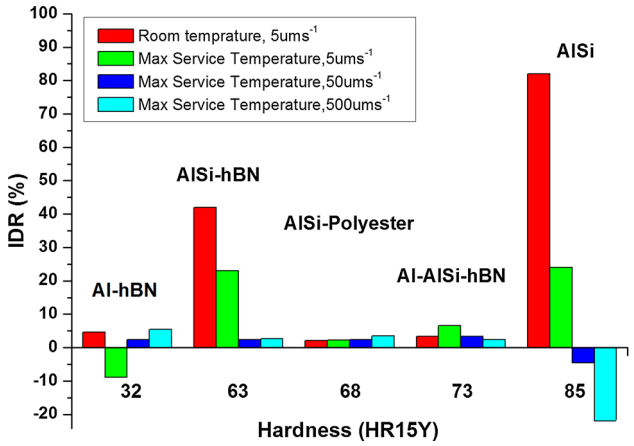

Fig. 7 IDR values of abradable coatings rubbed by T6Al4V blades

was found. The wear tracks are longer with a regular shape. Meanwhile, transfer of AlSi coating material to the blade tip occurs, the blade tip was found buried in the transferred coating material, and the thickness of the transferred coating material increased as increasing the incursion rate.

Figure 5 illustrates the surface morphology of the Al-hBN, AlSi-polyester and Al-AlSi-hBN coatings after abradability tests, respectively. Three coatings can be cut well by T6Al4V blades both at the room and high temperatures. Blade tip wear is slight, and blade material transfer to coating can hardly be found on the coating wear tracks. The shape of coating wear tracks is regular, and the wear track surfaces are relatively smooth and even which revealed a good abradability. In Fig. 5, the localized collapse of wear track borders can be found on Al-hBN coating, and it was caused by rig vibration at high velocity conditions which is a common phenomenon for very soft coatings.

The surface morphology of AlSi-hBN coating after abradability tests is shown in Fig. 6. A 5-μm s^{-1} incursion rate created short saw teeth-like wear tracks at both of the room and high temperatures, which are related to a poor abradability. Blade tip wear can be recognized by light reflection color of the dummy blade tip. The wear tracks tended to be more regular and longer with increasing incursion rates, resulted in a better abradability and reduced blade tip wear.

IDR for each abradability test was calculated, and the results were plotted to coating hardness in Fig. 7. It can be seen that the AlSi coating exhibits worst abradability in the five coatings. The IDR value of AlSi coating at the room temperature is 85% which means 85% wear from blade tip and 15% from coating wear in the full incursion process. When the testing temperature was increased to 450 °C, the blade wear was getting reduced. AlSi coating exhibits good abradability at an incursion rate of 50 μm/s, only slight coating transfer occurred. While the incursion rate was increased to 480 μm/s, IDR value reached −22%, resulting in a heavy AlSi coating transfer to the blade tip.

AlSi-hBN coating exhibits poor abradability at low incursion rates both at the room temperature and high temperature; then, the IDR values are 42 and 23%, respectively. With increasing incursion rates at high temperature, the abradability of AlSi-hBN coating was enhanced significantly; also, the IDR values close to zero. AlSi-polyester, Al-AlSi-hBN and Al-hBN coatings exhibited good abradability, and the IDR values of those three coatings are close to zero under all testing conditions.

In Fig. 7, it can also be found that hardness variation of coatings functioned on abradability irregularly.

Coatings Microstructure

Figure 8 gives the cross-sectional SEM photographs of five tested coating samples in the as-sprayed state. The five coatings consist mainly of metal matrix and secondary fillers. The main differences on the microstructure images are the secondary filler dimension and area fraction, summarized in Table 4. Due to their similar contrast to secondary fillers in the SEM image, pores and oxides in the coatings are not distinguishable from the fillers.

Discussion

AlSi coating is a conventional abradable coating, and still being used in certain modern turboshaft engines. From the testing results in the work, it can be seen that AlSi coating cannot be cut into by Ti6Al4V blades at the room temperature. But, AlSi coating can provide an acceptable abradability rubbed by Ti-6Al-4V blades under an

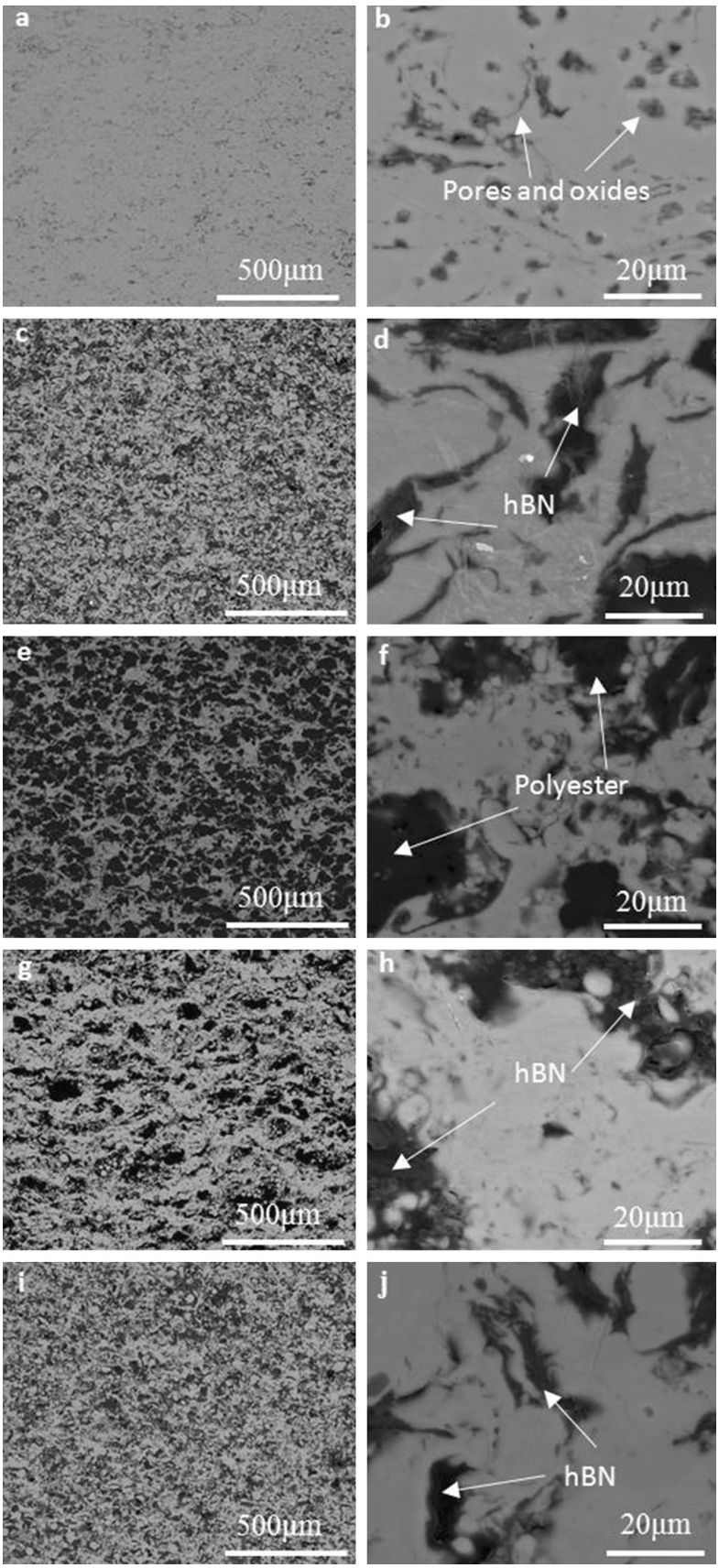

Fig. 8 Cross-sectional SEM photographs of coatings

Table 4 Secondary filler area fraction and dimension of tested coatings

Coating name	Filler type	Filler dimension, μm	Filler area fraction, %
AlSi	Oxides and pores	<10	8
Al-hBN	hBN, oxides and pores	10-50	33
AlSi-polyester	Polyester, oxides and pores	10-50	35
AlSi-hBN	hBN, oxides and pores	50-100	52
Al-AlSi-hBN	hBN, oxides and pores	50-200	37

enhanced temperature up to 450 °C, even with a dense microstructure. Al-12Si eutectic alloy has a melting temperature of 540 °C approximately; meanwhile, the melting temperature of Ti6Al4V alloy is 1660°°C. Therefore, AlSi should be much softer than Ti-6Al-4V alloy at 450 °C, which shall make Ti-6Al-4V blades easy cutting into the dense AlSi coating.

While the abradability of AlSi coating is not satisfied even at 450°°C due to severe blade wear at low incursion rate and heavy coating transfer at high incursion rate. An incursion rate of 5 μm/s is the most severe testing condition in the work. With a blade tip velocity of 300 m/s, a test rig spindle speed of 12,000 rpm was used. In the case, the scratching frequency of blade tip on the coating surface reached as high as 200 times/s. Under these conditions, the cutting force from blade tips is relatively low due to the low incursion rate and may not be able to remove coating material efficiently; then, a high frequency dry sliding wear occurred between the blade tip and coating surface. Friction heating generated from the high frequency dry sliding wear may lead to molten wear of the blade tips. With increasing incursion rates, cutting forces from the blade tip are enhanced and the blade tip can remove coating material more efficiently. Then after, the plastic debris from the AlSi coating will cause a heavy coating transfer under a higher cutting pressure at high incursion rates.

The other four coatings which contain secondary fillers perform much better than AlSi in general. Apparently, the addition of secondary fillers can weaken coating strength and reduce the ductility of coating debris, thereby increasing coating abradability. The abradability testing results show that coating abradability improves with the increase in secondary filler volume fraction. The results also show that, not only the added amount but also the diameter of secondary fillers imposed an important influence on coating abradability.

For a similar level of secondary filler addition, AlSi-hBN coating which contains coarse hBN filler performed much worse than Al-hBN and Al-AlSi-hBN coatings which contain fine hBN filler at the incursion rate of 5 μm/s. Clearly, filler spacing in the fine filler sample shall be shorter, compared with a coarse filler specimen, which means a thinner metal matrix skeleton. At the incursion rate of 5 μm/s, the cutting force may be too small for Ti-6Al-4V blades to break coarse coating metal matrix skeleton of AlSi-hBN, which resulted in a severe blade tip wear. On the contrary, Al-hBN and Al-AlSi-hBN coatings with thinner metal matrix skeleton can be broken easily at the same conditions.

It is believed that the results are meaningful for abradable coating design. The addition of secondary fillers improves coating abradability, but may induce some negative results such as reduced coating bond strength and erosion resistance, and so, there is a limitation on fillers addition. From the results, it can be seen that it is possible to increase coating abradability by reducing filler dimensions and keeping the filler content unchanged. But more work should be carried out to study the influence of filler dimension on coating properties such as bonding strength and erosion resistance.

It should be acknowledged that all of the five abradables can be deposited and have a rather wide range of hardness/microstructure, and even the present work only examined a single point on the hardness curve for each abradable. At the hardness levels and microstructures selected in the work, it was found that coating hardness is not a unique factor to describe coating abradability performance of different coatings. The investigation also revealed that the fine filler-added coatings exhibited much better abradability than those with coarse filler under the same addition level. To understand the relationship between coating chemical composition, microstructure and abradability well, more works should be carried out on the coating samples with variant hardness and microstructures.

Conclusions

The abradability of five aluminum-based abradable coatings rubbed by Ti6Al4V dummy blades was tested with a high-speed and high-temperature test rig. The results show that AlSi-polyester, Al-hBN and Al-AlSi-hBN coatings exhibited good abradability under all testing conditions, and the IDR value is in a range of −8.9-6.5%. AlSi-hBN coating showed poor abradability at low incursion rate and enhanced abradability at high incursion rates. AlSi coating performed worst as the severe blade tip wear at low incursions (IDR value up to 82%) and coating transfer to

blade tip at high incursion rates (IDR value up to −22%). The addition of secondary filler to aluminum-based coating is necessary for an improved abradability. The area fraction and dimension of the secondary filler play important role in coating abradability. In general, the more the secondary filler in coating, the better the abradability. When the secondary filler addition is on a similar level in volume percent, the coatings with fine filler performed better than those with coarse filler. Shorter filler spacing in the fine filler samples is concluded as the reason for the better abradability. It is also noticed that coating hardness is not a unique factor related to the practical abradability performance of coatings.

References

1. R.E. Chupp, R.C. Hendricks, S.B. Lattime, and B.M. Steinetz, Sealing in Turbomachinery, *J. Propul. Power*, 2006, **22**(2), p 313-349
2. S. Wilson, Thermally sprayed abradable coating technology for sealing in gas turbines, The Future of Gas Turbine Technology, 6th International Conference, 17-18 October 2012, Brussels, Belgium, Paper ID Number 51.
3. W.D. Marscher and C. Osborne, Abradable Turbine Shroud Development, Final Report, TN-343, Creare Inc., 1983.
4. N. Hopkins, The Black Art of Abradable Coatings, *PEI*, 2007, **15**(4), p 50-52
5. X. Ma and A. Matthews, Investigation of Abradable Seal Coating Performance Using Scratch Testing, *Surf. Coat. Technol.*, 2007, **202**(4-7), p 1214-1220
6. R.E. Johnston and W.J. Evans, Freestanding Abradable Coating Manufacture and Tensile Test Development, *Surf. Coat. Technol.*, 2007, **202**(4-7), p 725-729
7. R.E. Johnston, The Sensitivity of Abradable Coating Residual Stresses to Varying Material Properties, *J. Thermal Spray Technol.*, 2009, **18**(5), p 1004-1013
8. R. Bolot and J.-L. Seichepine, Predicting the Thermal Conductivity of AlSi/Polyester Abradable Coatings: Effects of the Numerical Method, *J. Thermal Spray Technol.*, 2011, **20**(1), p 39-47
9. M. Dorfman, U. Erning, and J. Mallon, Gas Turbines Use 'Abradable' Coatings for Clearance-Control Seals, *Seal. Technol.*, 2002, **97**, p 7-8
10. R.K. Schmid, New High Temperature Abradables for Gas Turbines (Diss. ETH No. 1223, 1997), p. 83-89.
11. R.C. Schwab, Program to Develop Sprayed, Plastically Deformable Compressor Shroud Seal Materials, 1979, NAS3-20054, CR159741.
12. E. Irissou, A. Dadouche, and R.S. Lima, Tribological Characterization of Plasma-Sprayed CoNiCrAlY-BN Abradable Coatings, *J. Thermal Spray Technol.*, 2014, **23**(1), p 252-261
13. D. Aussavy, R. Bolot, and G. Montavon, YSZ-Polyester Abradable Coatings Manufactured by APS, *J. Thermal Spray Technol.*, 2016, **25**(1), p 252-263
14. T.A. Taylor, B.W. Thompson, and W. Aton, High Speed Rub Wear Mechanism in IN-718 Vs. NiCrAl-Bentonite, *Surf. Coat. Technol.*, 2007, **202**(4-7), p 698-703
15. J. Stringer and M.B. Marshall, High Speed Wear Testing of An Abradable Coating, *Wear*, 2012, **294-295**, p 257-263
16. H. Wang, Criteria for Analysis of Abradable Coatings, *Surf. Coat. Technol.*, 1996, **79**(1), p 71-75
17. U. Bardi, C. Giolli, A. Scrivani, and G. Rizzi, Development and Investigation on New Composite and Ceramic Coatings as Possible Abradable Seals, *J. Thermal Spray Technol.*, 2008, **17**(5), p 805-811
18. C.-J. Li, J. Zou, H.-B. Huo, and J.-T. Yao, Microstructure and Properties of Porous Abradable Alumina Coatings Flame-Sprayed with Semi-molten Particles, *J. Thermal Spray Technol.*, 2016, **25**(1), p 264-272
19. R.K. Schmid, F. Ghasripoor, M. Dofman, and X. Wei, An Overview of Compressor Abradables, Proc. 1st International Thermal Spray Conference, May 8-11, 2000 (Montreal, Canada), p 1087-1093.
20. N. Fois and M.B.Marshall. Stringer, Adhesive Transfer in Aeroengine Abradable Lings Contact, *Wear*, 2013, **304**, p 202-210
21. W.H. Xue, S.Y. Gao, and D.L. Duan, Material Transfer Behavior Between a Ti6Al4V Blade and An Aluminum Hexagonal Boron Nitride Abradable Coating During High-Speed Rubbing, *Wear*, 2015, **322-323**, p 76-90
22. M. Bounazef, S. Guessasma, and B.A. Saadi, The Wear, Deterioration and Transformation Phenomena of Abradable Coating BN-SiAl-Bounding Organic Element, Caused by the Friction between the Blades and the Turbine Casing, *Mater. Lett.*, 2004, **58**(27-28), p 3375-3380